Artical ID:1006-3471(2012)02-0162-07

Electrochemical Preparation of Nanostructural Pt-Ni and Pd-Ni Films for Ethanol Electro-Oxidation

YAO Chen-zhong[1*], MA Hui-xuan[1], WEI Bo-hui[2]
(1. *Department of Applied Chemistry, Yuncheng University, Yuncheng* 044000, *Shanxi, China*;
2. *Library of Yuncheng University, Yuncheng* 044000, *Shanxi, China*)

Abstract: The Pt-Ni and Pd-Ni films were successfully prepared on Ti substrates by electrodeposition method. The porous Pt-Ni nanoflakes appeared to be uniform with the thickness of the slices about 10 ~ 20 nm. The porous Pd-Ni nanoparticles with a flower shape appeared to be uniform with the diameters of 50 ~ 60 nm. The XRD patterns also indicated that the Pd-Ni and Pt-Ni nanostructures have the poor crystallinity. The onset potentials of ethanol oxidation were negatively shifted to −0.74 V on Pt-Ni electrodes and −0.71 V on Pd-Ni electrodes, respectively. Addition of Ni could enhance catalytic activities and antitoxic properties of Pt, as well as the electro-catalytic activities of Pd for ethanol oxidation in alkaline media.

Key words: nanostructure; electrodeposition; porous structure; ethanol electro-oxidation
CLC Number: O646.21 **Document Code**: A

Nanoparticles (NPs) have been widely studied in many research areas involving microelectronic devices, photocatalysts, electro-catalysts, and biosensor design[1]. It is well known that the template-free electrodeposition is one of the most efficient methods for the preparation of NPs due to its rapidity and facility, allowing easy control of the nucleation and growth of metal NPs[2-4]. Our group has done a lot of work in preparing RE-TM, TM-Bi and Zn-Sb alloy films by electrodeposition[5-7]. The electrode surface morphology has an important effect on the property of redox active species during an electrochemical experiment[8]. So, the most attention has been paid on the various shapes of nanoparticles supported on the electrodes[1,9].

Ethanol has higher energy density and lower toxicity compared to methanol[10]. The ethanol electro-oxidation can be applied to direct ethanol fuel cells (DAFCs) and ethanol sensors. Much attention has been focused on searching much cheaper, stronger antitoxic and more catalytically active catalysts[11-12]. Pt has been extensively investigated as the electro-catalyst for ethanol electro-oxidation in acid media[13] although pure Pt has a very low activity. If ethanol electro-oxidation proceeds in alkaline rather than acidic media, the kinetics will be significantly improved[14]. A lot of work has been done to study the electro-oxidation of ethanol on Pt-based catalysts in alkaline media. Pd is a better electro-catalyst for ethanol oxidation in alkaline media[15], too. However, the high price and limited supply of Pt and Pd have become a bottleneck restricting the development of DAFCs.

One effective approach to the cost reduction is to reduce the content of the Pt and Pd catalysts. For decades, significant progress has been made in the development of other metal or metal oxide modified Pt and

Received: 2011-11-06, Revised: 2011-12-09 * Corresponding author, Tel:(86-359)2090394, E-mail:yaochzh1999@126.com
This work was supported by NSFC (No. 51101138, No. 20873184, No. 90923008), S & T Project of Shanxi Department of Education (No. 20111024), Innovation and Entrepreneurship for College Students Project in Shanxi Province (No. 2011343) and Young Teacher Starting-up Research of Yuncheng University (No. YQ-2010013)

Pd electro-catalysts for ethanol oxidation in alkaline media[16-17]. Here, the porous structural Pt-Ni and Pd-Ni films supported on Ti substrates were prepared by electro-deposition method and used as catalysts for ethanol electro-oxidation in alkaline media.

1 Experimental

All the electrochemical measurements were carried out in a three-electrode cell using CHI 700C electrochemical workstation (CHI Instrument, Inc., USA) at 298 K in a temperature-controlled water bath. A platinum substrate (3.0 cm^2) and a saturated calomel electrode (SCE, 0.241 V vs. RHE) were used as counter and reference electrodes, respectively. A salt bridge was used between the cell and the reference electrode. The films were analyzed by scanning electron microscope (SEM, Quanta 400), energy dispersive X-ray spectrometer (EDX, OXFOXD-INCA) and X-ray diffraction spectrometer (XRD, D/MAX 2200 VPC). The metal contents in the catalysts were also dissolved by aqua regia, diluted by using acidific water, and determined by the inductively coupled plasma-atomic emission spectrometry (ICP-AES, IRIS (HR)). The Pt-Ni nanoparticles were obtained in a mixed solution containing 0.01 mol · L^{-1} H_2PtCl_6 + 0.007 mol · L^{-1} $NiCl_2$ + 0.1 mol · L^{-1} KCl + 0.5 mol · L^{-1} citric acid on Ti substrates under 0.1 C · cm^{-2} charge loading by galvanostatic electrodeposition. While the Pd-Ni nanoparticles were obtained in solutions containing 0.01 mol · L^{-1} $PdCl_2$ + 0.005 mol · L^{-1} $NiCl_2$ + 0.1 mol · L^{-1} KCl + 0.5/0.1 mol · L^{-1} citric acid on Ti substrates under 0.1 C · cm^{-2} charge loading with a current density of 2 mA · cm^{-2}. The test solutions contained KOH and CH_3CH_2OH (both analytical reagents) with various concentrations. CVs were measured at a potential sweep rate of 50 mV · s^{-1}. Prior to and during the tests, the solutions were purged with high-purity nitrogen gas (99.999%).

2 Results and Discussion

Fig. 1 (A, B) shows the SEM images of Pt-Ni nanoflakes supported on Ti substrates deposited with a current density of 1.0 mA · cm^{-2}. The distribution of nanoflakes appears to be uniform with a porous structure. The thickness of the nanoflake slice is about 10 ~ 20 nm. Fig. 1(C, D) show the SEM images of Pt-Ni films deposited with a larger current density of 2.0 mA · cm^{-2}. The morphologies of Pt-Ni films obtained with a higher current density exhibit nanocones with a thickness about 60 nm. The EDX and ICP-AES analysis results confirm that the atomic ratio of Pt and Ni are 51.4% and 48.6% in the thin films (Fig. 2A). The loadings of Pt and Ni are 0.032 and 0.011 mg · cm^{-2}, respectively. The XRD pattern of the as-deposited Pt-Ni nanoflakes is given in Fig. 2B. A broad peak with a low intensity is observed between 20 and 40 degrees, indicating the poor crystalline properties of the prepared deposits.

The SEM images of Pd-Ni nanoparticles supported on Ti substrates are also shown in Fig. 3. The porous nanostructures of flower type in Fig. 3(A, B) were obtained with 0.5 mol · L^{-1} citric acid and consisted of nanoparticles with the diameter of 50 ~ 60 nm. Decreasing concentration of citric acid to 0.1 mol · L^{-1}, the more compact nanoparticles were formed as shown in Fig. 3(C, D). The results demonstrate that metal size and morphology can be easily con -

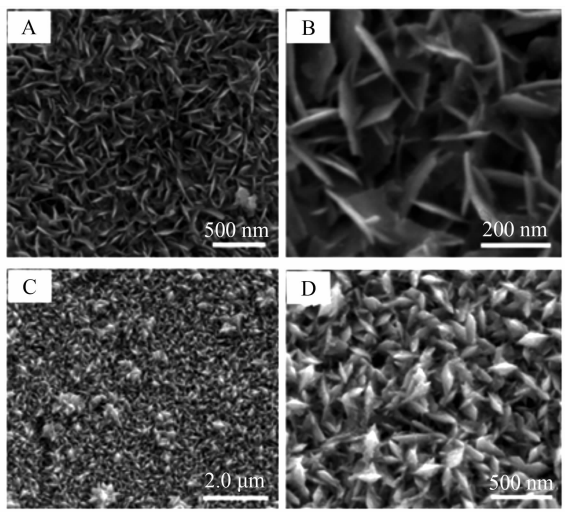

Fig. 1 SEM images of the Pt-Ni films prepared by galvanostatic electrodeposition in 0.01 mol · L^{-1} H_2PtCl_6 + 0.005 mol · L^{-1} $NiCl_2$ + 0.1 mol · L^{-1} KCl + 0.5 mol · L^{-1} citric acid under 0.1 C · cm^{-2} charge loading (A and B 1.0 mA · cm^{-2}; C and D 2.0 mA · cm^{-2})

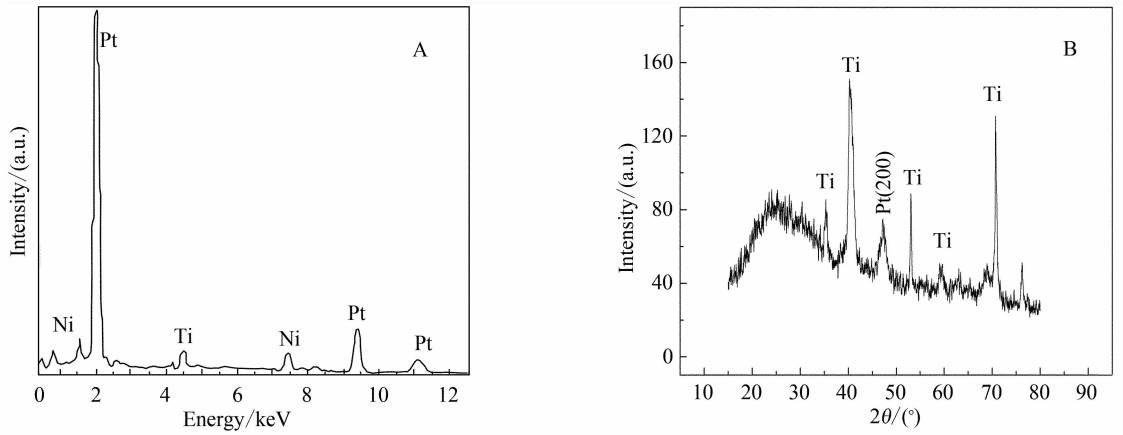

Fig. 2 EDX (A) and XRD (B) patterns of Pt-Ni nanoflakes prepared in 0.01 mol · L^{-1} H_2PtCl_6 + 0.005 mol · L^{-1} $NiCl_2$ + 0.1 mol · L^{-1} KCl + 0.5 mol · L^{-1} citric acid with a current density of 1.0 mA · cm^{-2} under 0.1 C · cm^{-2} charge loading

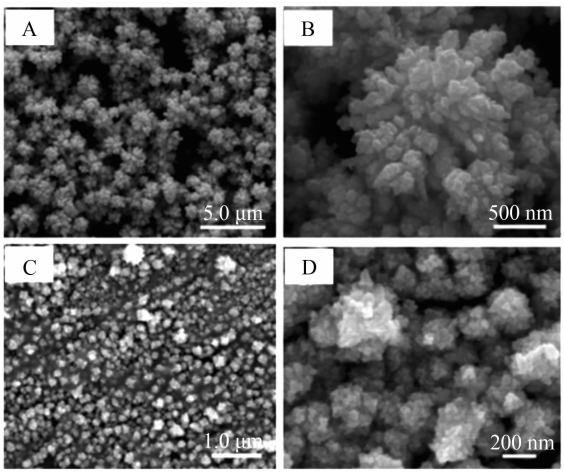

Fig. 3 SEM images of the Pd-Ni films prepared by 2.0 mA · cm^{-2} electrodeposition in 0.01 mol · L^{-1} $PdCl_2$ + 0.005 mol · L^{-1} $NiCl_2$ + 0.1 mol · L^{-1} KCl under 0.1 C · cm^{-2} charge loading (A and B with 0.5 mol · L^{-1} citric acid; C and D with 0.1 mol · L^{-1} citric acid)

trolled through regulating additive concentrations as demonstrated by Wang et al[18]. The composition of Pd-Ni nanoparticles shown in Fig. 3 (A) was also confirmed by EDX and ICP-AES analysis with the atomic ratio of Pd and Ni elements being 78.4% and 21.6% in the thin films (Fig. 4A). The loadings of Pd (0.043 mg · cm^{-2}) and Ni (0.007 mg · cm^{-2}) could be evaluated from EDX analyses. The XRD pattern in Fig. 4B also indicates the poor crystallinity of the as-deposited Pd-Ni nanoparticles.

Fig. 5 compares the cyclic voltammograms (CVs) obtained with different electrodes. In the presence of alcohol, an oxidation peak can be clearly observed for ethanol (Fig. 5B). The electrochemical active area (EAA) was calculated with the background lines. In 1.0 mol · L^{-1} KOH electrolyte solution (Fig. 5A), the anodic peaks appearing between −0.9 to −0.64 V may be originated from desorption of atomic hydrogen on Pt with an oxidation peak (a) at −0.84 V. Also, the anodic peak (−0.85 ~ −0.5 V) may be due to desorption of atomic hydrogen on Pd with an oxidation peak (a′) at −0.67 V[19]. Thus, the area of H-desorption on the CV curves represents the charge passed for H-desorption Q_H, and can be used to estimate the EAA of the electrode[20].

The EAA can be calculated according to the Eq. (1)

$$EAA = kQ_H/[M] \quad (1)$$

where [M] is the platinum and palladium loadings (mg · cm^{-2}) of the electrode. The current for measured hydrogen desorption has deducted the double layer charging. k represents the charge required to oxidize a monolayer of H_2 on bright Pt or Pd. The values of k is 0.21 on Pt electrodes[21] and 0.25 on Pd electrodes[22] represents the charge required to oxidize a monolayer of H_2 on bright Pt. The results in Tab. 1 show that the EAAs of Pt-Ni and Pd-Ni are smaller than those of Pt and Pd. This indicates that electrochemical oxidation of ethanol is more active on Pt-Ni and Pd-Ni electrodes than on Pt and Pd electrodes without increasing the EAAs of the electrodes. The

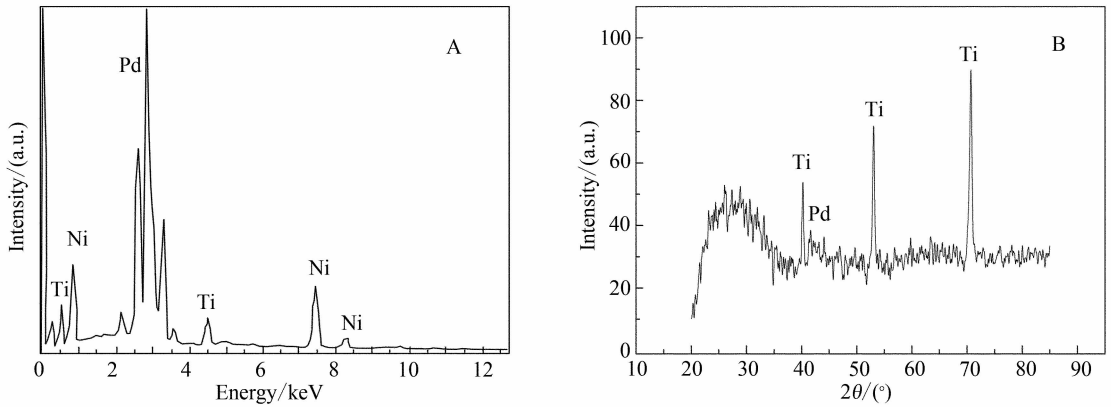

Fig. 4　EDX (A) and XRD (B) patterns of Pd-Ni nanoparticles prepared in 0.01 mol · L^{-1} $PdCl_2$ + 0.005 mol · L^{-1} $NiCl_2$ + 0.1 mol · L^{-1} KCl + 0.5 mol · L^{-1} citric acid with a current density of 2.0 mA · cm^{-2} under 0.1 C · cm^{-2} charge loading

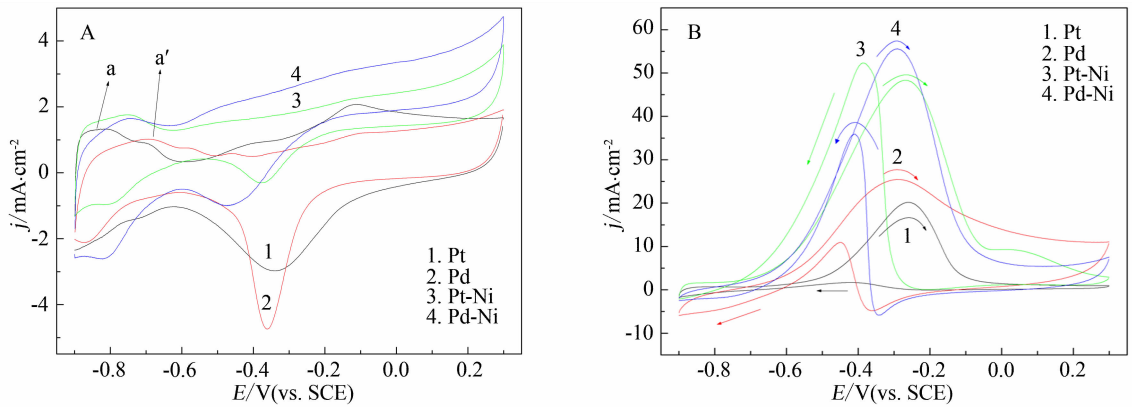

Fig. 5　CVs of the ethanol oxidation on Pt (Pt loading 0.051 mg · cm^{-2}), Pd (Pd loading 0.055 mg · cm^{-2}), Pt-Ni (Pt loading 0.032 and Ni loading 0.011 mg · cm^{-2}) and Pd-Ni (Pd loading 0.043 and Ni loading 0.007 mg · cm^{-2}) in a N_2-saturated 1.0 mol · L^{-1} KOH (A) and 1.0 mol · L^{-1} KOH + 1.0 mol · L^{-1} ethanol (B) solutions at a sweep rate of 50 mV · s^{-1}

Tab. 1　The H-desorption Q_H and the EAAs of different electrodes for ethanol oxidation

Electrodes	Pt	Pd	Pt-Ni	Pd-Ni
Q_H/ mC · cm^{-2}	1.6	1.7	0.9	0.8
EAA/m^2 · g^{-1}	7	6	6	4

decrease of EAAs by adding Ni can be attributed to that the places of Pt and Pd atoms are substituted by Ni atoms.

The composition and electro-catalytic performance for ethanol oxidation of Pt-Ni and Pd-Ni films supported on Ti substrates are summarized in Tab. 2 and Tab. 3, respectively. The onset potential (E_o) of ethanol oxidation on Pt was −0.54 V and shifted negatively to −0.74 V on Pt-Ni electrodes (Tab. 2). Similar phenomena were observed for ethanol oxidation on Pd and Pd-Ni electrodes. The E_o was −0.61 V on Pd, while −0.71 V on Pd-Ni (Tab. 3). Negative shift of E_o (≥0.1 V) for anodic reaction is significant for liquid fuel cells. The changes in E_o indicate an improvement in the kinetics caused by the synergistic effects between Pt/Pd and Ni. The current density of ethanol oxidation at −0.4 V on Pt-Ni was 33.1 mA · cm^{-2}, which is higher than that on Pt (8.8 mA · cm^{-2}), while 39.0 mA · cm^{-2} on Pd-Ni and 21.1 mA · cm^{-2} on Pd. The activities of ethanol electro-oxidation on Pt and Pd electrodes were significantly increased by the addition of Ni. The stability of ethanol oxidation on the above electrodes was investigated at a potential of −0.4 V (Fig. 6). The oxidation current

Tab. 2 The composition and electro-catalytic performance for ethanol oxidation of Pt-Ni films prepared by electrodeposition using 1 mA · cm^{-2} to get 0.1 C · cm^{-2} in solutions composed of 0.1 mol · L^{-1} KCl, 0.5 mol · L^{-1} citric acid, 0.01 mol · L^{-1} H_2PtCl_6 and different concentrations of $NiCl_2$

Concentration of Ni (II)/ mmol · L^{-1}	Atomic ratio Pt/Ni	Pt/Ni Loading/ mg · cm^{-2}	E_o/V	j(at −0.4 V)/ mA · cm^{-2}
0	100/0	0.051/0	−0.54	8.8
5.0	51.4/48.6	0.034/0.010	−0.74	27.1
7.0	47.0/53.0	0.032/0.011	−0.74	33.1
10.0	40.8/59.2	0.029/0.013	−0.64	13.5

Tab. 3 The composition and electro-catalytic performance for ethanol oxidation of Pd-Ni films prepared by electrodeposition using 2 mA · cm^{-2} to get 0.1 C · cm^{-2} in solutions composed of 0.01 mol · L^{-1} $PdCl_2$, 0.1 mol · L^{-1} KCl, 0.5 mol · L^{-1} citric acid and different concentrations of $NiCl_2$

Concentration of Ni(II)/ mmol · L^{-1}	Atomic ratio Pd/Ni	Pd/Ni loading/ mg · cm^{-2}	E_o/V	j(at −0.4 V)/ mA · cm^{-2}
0	100/0	0.055/0	−0.61	21.1
2.5	87.7/12.3	0.048/0.004	−0.65	29.7
3.3	78.4/21.6	0.043/0.007	−0.71	39.0
5.0	59.6/40.4	0.033/0.012	−0.66	32.4

densities were larger on Pt-Ni and Pd-Ni than those on Pt and Pd at the end of the tests. This indicates that Ni can enhance the stability and poisoning tolerance of Pt and Pd electro-catalysts for ethanol oxidation.

The optimization of the atomic ratios of Ni to Pt or Pd in these electro-catalysts was conducted by changing the $NiCl_2$ concentration and recording the onset potential and current densities at −0.4 V during the ethanol electro-oxidation. The best electrodeposited conditions for Pt-Ni films were in a solution of 0.01 mol · L^{-1} H_2PtCl_6 + 0.007 mol · L^{-1} $NiCl_2$ + 0.1 mol · L^{-1} KCl + 0.5 mol · L^{-1} citric acid on Ti with 1 mA · cm^{-2}, while for Pd-Ni films in a solution of 0.01 mol · L^{-1} $PdCl_2$ + 0.005 mol · L^{-1} $NiCl_2$ + 0.1 mol · L^{-1} KCl + 0.5 mol · L^{-1} citric acid with 1 mA · cm^{-2}.

The alcohol electro-oxidation on Pt-Ru catalyst supported on C substrates is explained as a bi - functional mechanism[23]. It is possible that Ni functions as Ru does in Pt - Ni and Pd - Ni catalysts. Some researchers have found that Pt-Ni nanoparticles show a shift in the Pt 4f peak in a Pt-Ni based alloy structure, so called the electronic effect[24]. Enhanced activity of alcohol electro-oxidation such as lower onset potential and improved stability may be responsible for the change in the electronic properties of Pt and

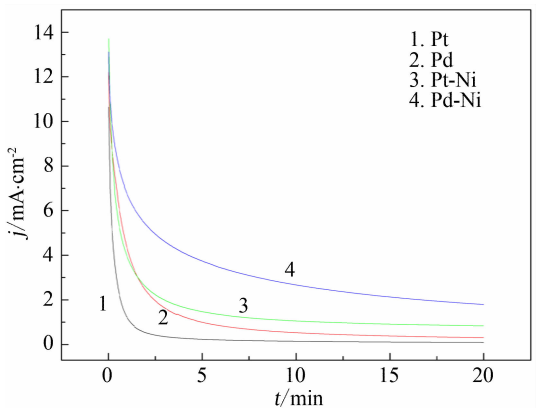

Fig. 6 Current density ~ time curves for ethanol oxidation at −0.4 V on Pt (0.051 mg · cm^{-2}), Pd (0.055 mg · cm^{-2}), Pt-Ni (Pt 0.032 and Ni 0.011 mg · cm^{-2}) and Pd-Ni (Pd 0.043 and Ni 0.007 mg · cm^{-2}) electrodes in 1.0 mol · L^{-1} KOH solution containing 1.0 mol · L^{-1} ethanol

Pd in Pt-Ni and Pd-Ni. On the other hand, hydrous RuO_2 is a more active catalyst for alcohol oxidation than Ru^0 being a part of bimetallic Pt-Ru alloy[25]. The presence of hydrous RuO_2 ($RuO_{2-\delta}(OH)_\delta$) could play an important role being a donor of the oxygen-containing species that promote the CO to CO_2 oxidation. Non-noble oxides were shown to be active sites for the formation of oxygen-containing species as Ru[26]. The Ni is easily oxidized in air and alkaline solution. The Ni and Ni oxide may co-exist in the prepared Pt-Ni and Pd-Ni films. The interactions of metal particles with oxide supports can radically enhance the performance of supported catalysts. Vayssilov et al explored Pt-CeO_2 catalysts, and suggested that there are two types of oxidative metal-oxide interaction: 1) electron transfer from the Pt nanoparticle to the support; 2) oxygen transfer from ceria to Pt[27-28]. For Pt-Ni and Pt-Pd electrocatalysts, the addition of Ni and formation of Ni oxides can significantly increase the activity for alcohol electro-oxidation.

3 Conclusions

The porous nanostructured Pt-Ni and Pd-Ni films supported on Ti substrates were successfully prepared by electrochemical deposition method. The porous Pt-Ni nanoflakes appeared to be uniformly distributed with the thickness of slice about 10 ~ 20 nm. The porous Pd-Ni nanoparticles with a flower shape appeared to be uniformly distributed with the diameter of 50 ~ 60 nm. The activity of the catalysts for ethanol electro-oxidation was significantly increased by the addition of Ni. The optimized condisitons for electro-depositions of Pt-Ni films were in a solution of 0.01 mol · L^{-1} H_2PtCl_6 + 0.007 mol · L^{-1} $NiCl_2$ + 0.1 mol · L^{-1} KCl + 0.5 mol · L^{-1} citric acid on Ti with 1 mA · cm^{-2}, while for those of Pd-Ni films in a solution of 0.01 mol · L^{-1} $PdCl_2$ + 0.05 mol · L^{-1} $NiCl_2$ + 0.1 mol · L^{-1} KCl + 0.5 mol · L^{-1} citric acid with 1 mA · cm^{-2}. The activities for ethanol electrochemical oxidation on Pt-Ni and Pd-Ni electrodes were higher than those on Pt and Pd electrodes without increasing the EAAs. The change of the onset potential shows an improvement in the kinetics caused by the synergistic effects between Pt/Pd and Ni.

References:

[1] Scavetta E, Stipa S, Tonelli D. Electrodeposition of a nickel-based hydrotalcite on Pt nanoparticles for ethanol and glucose sensing[J]. Electrochemistry Communications, 2007, 9(12): 2838-2842.

[2] Nielsch K, Müller F, Li A P, et al. Uniform nickel deposition into ordered alumina pores by pulsed electrodeposition[J]. Advanced Materials, 2000, 12(8): 582-586.

[3] Ji X B, Banks C E, Xi W, et al. Edge plane sites on highly ordered pyrolytic graphite as templates for making palladium nanowires via electrochemical decoration [J]. The Journal of Physical Chemistry B, 2006, 110 (45): 22306-22309.

[4] Welch C M, Compton R G. The use of nanoparticles in electroanalysis: A review[J]. Analytical and Bioanalytical Chemistry, 2006, 384(3): 601-619.

[5] Liu P, Guo X A, Huang H, et al. The growth of Zn-Sb nanowires by heat treatment of Zn-Sb nanoparticles obtained by electrodeposition [J]. Advanced Materials, 2006, 18(14): 1873-1876.

[6] Li G R, Liu G K, Tong Y X. Electrochemical preparation of Yb-Bi thin film in dimethylsulfoxide[J]. Electrochemistry Communications, 2004, 6(5): 441-446.

[7] Liu P, Du Y P, Yang Q Q, et al. Electrochemical behavior of Fe(II) in acetamide-urea-NaBr-KBr melt and magnetic properties of inductively codeposited Nd-Fe film[J]. Electrochimica Acta, 2006, 52(2): 710-714.

[8] Wildgoose G G, Chevallier F G, Xiao L, et al. Designer interfaces: Diffusional protection of electrodes using chemical architectures[J]. Journal of Materials Chemistry, 2006, 16(42): 4103-4106.

[9] Streeter I, Compton R G. Diffusion-limited currents to nanoparticles of various shapes supported on an electrode; spheres, hemispheres, and distorted spheres and hemispheres[J]. The Journal of Physical Chemistry C, 2007, 111(49): 18049-18054.

[10] Jiang Q, Jiang L H, Wang S L, et al. A highly active Pt-Ni/C electrocatalyst for methanol electro-oxidation in alkaline media[J]. Catalysis Communications, 2010, 12(1): 67-70.

[11] Cao L, Scheiba F, Roth C, et al. Novel nanocomposite Pt/RuO_{2-x} H_2O/carbon nanotube catalysts for direct methanol fuel cells[J]. Angewandte Chemie International Edition, 2006, 45(32): 5315-5319.

[12] Castro Luna A M, Bonesi A, Triaca W E, et al. Pt-Fe cathode catalysts to improve the oxygen reduction reaction and methanol tolerance in direct methanol fuel cells[J]. Journal of Solid State Electrochemistry, 2008, 12(5): 643-649.

[13] Maiyalagan T, Nawaz Khan F. Electrochemical oxidation of methanol on Pt/V_2O_5-C composite catalysts [J]. Catalysis Communications, 2009, 10 (5): 433-436.

[14] Kang J Q, Ma W T, Wu J J, et al. A novel catalyst Pt@NiPcTs/C: Synthesis, structural and electro-oxidation for methanol [J]. Catalysis Communications, 2009, 10 (8): 1271-1274.

[15] Singh R N, Singh A, Anindita. Electrocatalytic activities of binary and ternary composite electrodes of Pd, nanocarbon and Ni for electro-oxidation of methanol in alkaline medium[J]. Journal of Solid State Electrochemistry, 2009, 13(8): 1259-1265.

[16] Chu D B, Wang J, Wang S X, et al. High activity of Pd-In_2O_3/CNTs electrocatalyst for electro-oxidation of ethanol[J]. Catalysis Communications, 2009, 10(6): 955-958.

[17] Xu C W, Shen P K. Novel $Pt/CeO_2/C$ catalysts for electrooxidation of alcohols in alkaline media [J]. Chemical Communications, 2004, (19): 2238-2239.

[18] Wang H L, Li W G, Jia Q X, et al. Tailoring conducting polymer chemistry for the chemical deposition of metal particles and clusters [J]. Chemistry of Materials, 2007, 19(3): 520-525.

[19] Pattabiraman R. Effects of small MoO_3 additions on the properties of nickel catalysts for the steam reforming of hydrocarbons[J]. Applied Catalysis A: General, 1997, 153(1/2): 9-20.

[20] Pozio A, De Francesco M, Cemmi A, et al. Comparison of high surface Pt/C catalysts by cyclic voltammetry [J]. Journal of Power Sources, 2002, 105(1): 13-19.

[21] Liu Y, Chen J, Zhang W M, et al. Nano-Pt modified aligned carbon nanotube arrays are effcient, robust, high surface area electrocatalysts[J]. Chemistry of Materials, 2008, 20 (8): 2603-2605.

[22] Liu Z, Yang Z L, Cui L, et al. Electrochemically roughened palladium electrodes for surface-enhanced raman spectroscopy: Methodology, mechanism, and application [J]. The Journal of Physical Chemistry C, 2007, 111 (4): 1770-1775.

[23] Yajima T, Wakabayashi N, Uchida H, et al. Adsorbed water for the electro-oxidation of methanol at Pt-Ru alloy[J]. Chemical Communications, 2003, (7): 828-829.

[24] Park K W, Choi J H, Sung Y E. Structural, chemical, and electronic properties of Pt/Ni thin film electrodes for methanol electrooxidation[J]. The Journal of Physical Chemistry B, 2003, 107(24): 5851-5856.

[25] Suffredini H B, Tricoli V, Vatistas N, et al. Electro-oxidation of methanol and ethanol using a $Pt\text{-}RuO_2/C$ composite prepared by the sol-gel technique and supported on boron-doped diamond[J]. Journal of Power Sources, 2006, 158(1): 124-128.

[26] Mukerjee S, McBreen J. An in situ X-ray absorption spectroscopy investigation of the effect of Sn additions to carbon-supported Pt electrocatalysts: Part I[J]. Journal of The Electrochemical Society, 1999, 146 (2): 600-606.

[27] Vayssilov G N, Lykhach Y, Migani Annapaola, et al. Support nanostructure boosts oxygen transfer to catalytically active platinum nanoparticles[J]. Nature Materials, 2011, 10(4): 310-315.

[28] Fu X Z, Liang Y, Chen S P, et al. Pt-rich shell coated Ni nanoparticles as catalysts for methanol electro-oxidation in alkaline media [J]. Catalysis Communications, 2009, 10(14): 1893-1897.

Pt-Ni 与 Pd-Ni 纳米薄膜的电化学制备和乙醇电催化性能研究

姚陈忠[1*], 马会宣[1], 卫博慧[2]

(1. 运城学院应用化学系, 山西 运城 044000; 2. 运城学院图书馆, 山西 运城 044000)

摘要: 通过电沉积法在 Ti 基体上制备具有纳米结构的 Pt-Ni 和 Pd-Ni 薄膜,前者呈纳米花瓣形状,厚度为 10 ~ 20 nm,后者主要由纳米颗粒组成,大小为 50 ~ 60 nm. XRD 测试结果显示,Pt-Ni 和 Pd-Ni 纳米薄膜结晶程度较差. 循环伏安法测试薄膜对乙醇电催化氧化的性能,结果表明 Pt-Ni 和 Pd-Ni 纳米薄膜可使乙醇起始氧化电位分别负移至 −0.74 V 和 −0.71 V,且在碱性介质中加 Ni 可提高催化剂的活性和抗毒化性能.

关键词: 纳米结构; 电沉积; 多孔结构; 乙醇电催化